

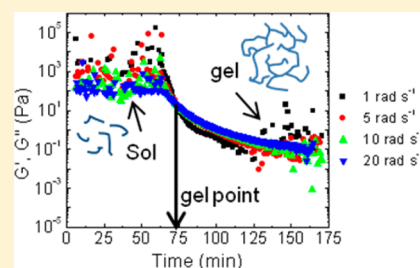
Gelation and Cross-Linking in Multifunctional Thiol and Multifunctional Acrylate Systems Involving an *in Situ* Comonomer Catalyst

Alina K. Higham,[†] Leah A. Garber,[‡] David C. Latshaw, II,[†] Carol K. Hall,[†] John A. Pojman,[‡] and Saad A. Khan^{*,†}

[†]Department of Chemical and Biomolecular Engineering, North Carolina State University, Raleigh, North Carolina 27695, United States

[‡]Department of Chemistry, Louisiana State University, Baton Rouge, Louisiana 70803, United States

ABSTRACT: Dynamic rheology in combination with Fourier transform infrared spectroscopy (FTIR) is used to examine the gelation kinetics, mechanism, and gel point of novel thiol–acrylate systems containing varying concentrations of an *in situ* catalyst. Gelation, as evidenced from the gel time determined using the Winter–Chambon criterion, is found to occur more quickly with increasing catalyst concentration up until a critical catalyst concentration of 22 mol %, whereupon the gel time lengthens. Such a minimum in gel time may be attributed to changes in the number of available reaction sites and percentage conversion required for gelation. Chemical conversions at the gel point measured for representative samples are consistent with theoretical values calculated using Flory–Stockmayer’s statistical approach, confirming our hypothesis. Relaxation exponents of 0.97 and fractal dimensions of 1.3 are calculated for all samples, consistent with coarse-grained discontinuous molecular dynamics (DMD) simulations. The elevated value of n may be due to the low molecular weight prepolymer. The relaxation exponent and fractal dimensions are invariable over all systems studied, suggesting the cross-linking mechanism remains unaffected by changes in catalyst concentration, allowing the gel time to be tailored by simply modulating the catalyst concentration.



INTRODUCTION

Polymerization via thiol–ene chemistry, the addition of a thiol group over a carbon–carbon double bond, has experienced a renewed interest in recent years. Materials synthesized using this approach are easily processed due to a solvent-free, rapid synthesis that can occur at room temperature and ambient pressure, yielding materials with high conversion¹ and uniform cross-link densities.^{2,3} As a result of these benefits, thiol–ene polymerization schemes are being used in various applications such as functionalization of nanoparticles,^{4–7} surface modification,^{8,9} and fabrication of biomaterials.¹⁰

Despite the strong interest, most thiol–ene systems currently investigated are produced via frontal polymerization^{11,12} or photoinitiation,^{13–15} which requires increased temperature or an external light source and photoinitiator, respectively. Additionally, these reactions produce radicals that may remain in the final product and leach into the body when used in biomedical applications. It has been shown that thiol–acrylate systems, created using thiol–ene chemistry by reacting a thiol functional group with an acrylate functional group,^{1,3,16} can be polymerized using primary,^{8,16} secondary, and tertiary amine catalysts in lieu of a photoinitiator.¹⁷ The amine catalyst acts as a base, thereby deprotonating the nucleophilic thiol group. Exploiting this benefit, Bounds et al. established a thiol–ene chemistry reaction to polymerize a thiol–acrylate network by introducing a tertiary amine as the effective *in situ* base catalyst/

comonomer.¹⁸ This novel system preserves all of the benefits of photopolymerized thiol–acrylate systems without the need of a photoinitiator and ultraviolet (UV) light source.

The *in situ* catalyst/comonomer is fabricated by reacting a secondary amine (diethylamine, DEA) with a trifunctional acrylate (pentaerythritoltriacylate, PETA), producing a tertiary amine, labeled as the catalyst/comonomer, as shown in Scheme 1. The catalyst/comonomer reacts with a trifunctional thiol (trimethylolpropanetri(3-mercaptopropionate), TMPTMP) via a Michael addition to create a thiol anion that is used to initiate polymerization, shown as initiation in Scheme 1. The thiolate anion initiator then reacts across the electron-deficient double bond of the acrylate functional group, present as a triacylate in this synthesis via another Michael addition, shown as propagation step 1 in Scheme 1. An electron-deficient carbon is created on the backbone, which can react with a trifunctional thiol to create another anion, which can continue the reaction, as shown in propagation step 2 in Scheme 1. The polymerization propagates via sequential chain transfer step growth after each addition, thereby having the attributes of an anionic step growth mechanism. Polymerization via a Michael addition mechanism alleviates concerns of unreacted radicals leaching

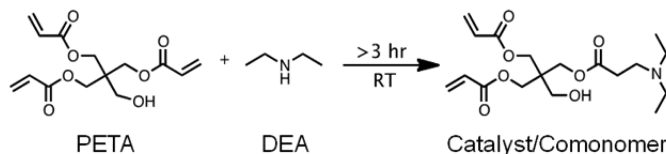
Received: October 19, 2013

Revised: December 21, 2013

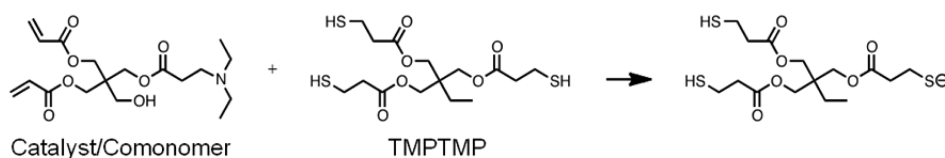
Published: January 6, 2014

Scheme 1. Polymerization Reaction for Triacrylate and Trithiol Monomers Containing an *in Situ* Amine Catalyst (Adapted from Ref 18)

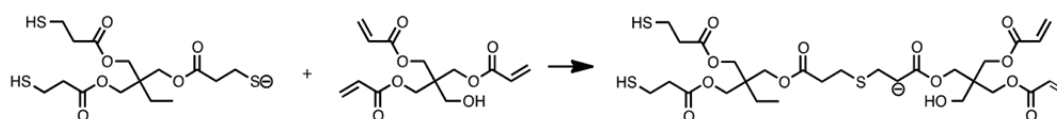
Formation of Catalyst/Comonomer



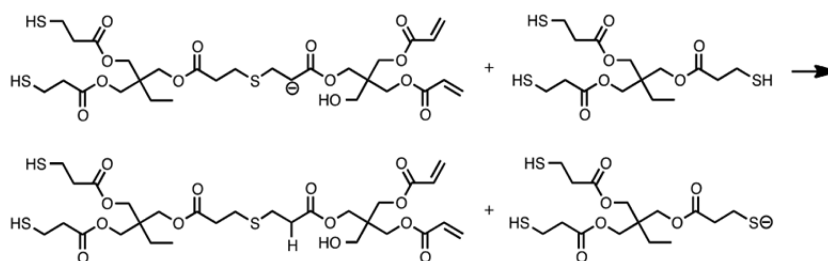
Initiation



Propagation 1 – Step Growth



Propagation 2 – Chain Transfer



from the final material, typical of photoinitiated thiol–acrylate systems. Additionally, postprocessing steps are not needed to remove the catalyst since it is incorporated into the thermoset network. This reaction scheme is ideal for use in biomedical applications, such as microfluidic devices,^{18,19} osteogenic foams for bone replacement,²⁰ and next-generation tissue scaffolds.^{13,21} For many of these applications, minimally invasive procedures, such as *in situ* polymerization, are desirable.

A fundamental understanding of the cross-linking mechanism and effects of material composition on gelation time are required before new polymerization schemes may be employed, especially since these systems transition from low viscosity liquids to high molecular weight networks over the course of time. In this study, we examine the gelation kinetics, mechanism, and microstructure of a thiolene system containing an *in situ* catalyst/comonomer as a function of material composition. The ability to alter or tune the gel point for these materials together with the incorporation of the catalyst/comonomer into the polymer network makes this system ideal for *in situ* polymerization applications. However, these systems are easily processed only at times before the gel point. It is therefore important to quantify and understand the role of material composition on the gel point so that a known processing window is readily available.

Small-amplitude dynamic oscillatory rheological techniques provide a powerful approach for monitoring the gelation of polymerizing systems. Information on the evolution of material

properties such as the elastic (G') and viscous (G'') moduli, as well as pinpointing the gel point can be gathered without disturbing the fragile microstructure.^{21–23} The gel point (GP) is defined as the moment at which the weight-average molecular weight diverges to infinity or an initial microstructure cluster first reaches from plate to plate.²² At this moment in time, the system has reached a critical extent of reaction ($p = p_c$), where p represents the fraction of functional groups lost. As the reaction continues to progress ($p > p_c$), the overall sample stiffness will increase as remaining molecules are integrated into the polymerizing network, resulting in a sample not soluble in even good solvents. Winter and Chambon have identified two rheological criteria for determining the gel point.^{23–25} Based on scaling theory, it has been shown that at the gel point, G' and G'' depend on frequency in the same manner. As a result, the ratio of G'' to G' , defined as $\tan \delta$, is independent of frequency at the gel point. This independence is graphically depicted as the point of intersection when monitoring $\tan \delta$ over time for varying frequencies. This relationship is mathematically shown in the equation

$$\tan \delta = \frac{G''}{G'} = \tan\left(\frac{n\pi}{2}\right) \quad (1)$$

where n is defined as the relaxation exponent, with a value in the range of $0 < n < 1$, and also represents the slope of the dynamic moduli at the gel point in a frequency spectrum. Although the Winter–Chambon method for gel point

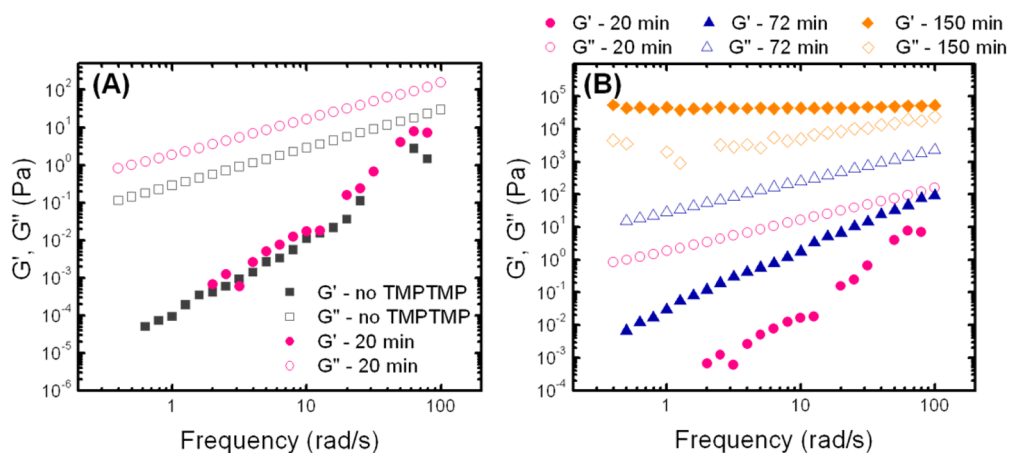


Figure 1. (A) Elastic (G') and viscous (G'') moduli of PETA with 34.2 mol % DEA with and without TMPTMP plotted as a function of frequency approximately 20 min after initial sample preparation. At this time, a microstructure large enough for detection has not formed as there is no change in G' . (B) G' and G'' of PETA with 34.2 mol % DEA at varying times after the addition of the trithiol. At 20 min, G'' is greater than G' for all frequencies, both showing frequency dependence, indicating the solution is still in the pregel state. At 72 min, both moduli have increased in magnitude, indicating a change in microstructure. At 150 min, G' is independent of frequency and at least 1 order of magnitude greater than G'' , indicating a cross-linked sample.

determination is well documented, it may require multiple experiments. Combining small-amplitude oscillatory dynamic rheology with Fourier transform mechanical spectroscopy (FTMS), a multiwave approach, provides a means to monitor the evolution of G' and G'' over time for several frequencies within one experiment.^{26,27}

In this study, we use dynamic rheology coupled with FTMS and the Winter–Chambon gel point criteria to characterize the evolution of novel trithiol–triacrylate systems utilizing an *in situ* catalyst/comonomer. We evaluate the gel point and evolution of the dynamic moduli as functions of time and diethylamine mol % concentration relative to acrylate functional groups. In addition, we combine the rheological technique with Fourier transform infrared spectroscopy (FTIR) to understand the relationship between percent conversion and gel strength. The properties of the microstructure (i.e., fractal dimension) at the gel point are analyzed using rheological techniques and correlated with computer modeling calculations.

EXPERIMENTAL SECTION

Materials. All materials were used as received. Pentaerythritol triacrylate (PETA) was obtained from Alfa Aesar. Trimethylolpropane tris(3-mercaptopropionate) (TMPTMP) and diethylamine (DEA) were purchased from Sigma-Aldrich.

Sample Preparation. The catalyst/comonomer solution was prepared by adding appropriate amounts of DEA to PETA in a glass vial containing a magnetic stir bar. DEA concentrations were calculated based on the molar ratio of amines with respect to acrylate functional groups. Once added, the vial was then capped, inverted several times, and stirred for a minimum of 3 h. When needed for rheology experiments, appropriate amounts of catalyst/comonomer were added into a glass vial with a magnetic stir bar. TMPTMP was then added to the solution in a stoichiometric 1:1 molar ratio of thiol to acrylate groups, based on the remaining amount of functional acrylate groups after the catalyst/comonomer reaction. The total volume of sample was maintained at 2 mL. The samples were then mixed gently for 2 min before loading the sample onto the rheometer.

Rheological Measurements. All rheology experiments were conducted using a TA Instruments (New Castle, DE) AR-G2 stress-controlled rheometer and a 40 mm, 2° cone and plate geometry. The absence of slip was verified by running experiments with various geometries and gap heights.²⁸ Measurements were obtained at 25 °C, which was controlled via water bath and temperature-controlled Peltier

plate. Solution gelling behavior was monitored using small-amplitude dynamic oscillatory time sweeps, where time zero represents the addition of TMPTMP. Multiwave experiments were performed with a fundamental frequency of 1 rad s⁻¹ with harmonics of 5, 10, and 20 and data acquisition intervals of 20 s. The stress applied to the sample was kept constant at 1 Pa, which was within the linear viscoelastic regime (LVR).

FTIR Spectroscopy. Thiol and acrylate conversions over time were calculated from changes in Fourier transform infrared spectroscopy (FTIR) (Bruker Tensor 27 FTIR Spectrometer) spectra. FTIR samples containing varying amine concentrations were prepared via the addition of TMPTMP initiator into the catalyst/comonomer solutions. The samples were mixed, and aliquots were deposited between two potassium bromide salt crystals. FTIR scans were run every 2 min for a 24 h period.

RESULTS AND DISCUSSION

Evolution of Thiol–Acrylate Polymerization. We first examine the role of a trifunctional thiol, trimethylolpropane tris(3-mercaptopropionate), henceforth referred to as TMPTMP, in the cross-linking process. Figure 1a shows the frequency spectra of the elastic (G') and viscous (G'') moduli at varying times before and after the addition of TMPTMP. Before the addition, samples contain only pentaerythritol triacrylate (PETA) and the *in situ* catalyst, which is formed from the addition of diethylamine (DEA) to PETA. Rheological experiments of these samples show typical solution behavior since the magnitude of G'' is greater than G' , and both are frequency dependent, scaling as follows: $G' \sim \omega^2$ and $G'' \sim \omega^1$. Note that the magnitude of G'' increases upon the addition of TMPTMP due to the viscous nature of the material. Measurements of the solution without the trithiol at longer times (data not shown) revealed a lack of change in the dynamic moduli, indicating an absence of microstructural change within the sample.

When TMPTMP is introduced into the sample, the dynamic moduli change as a function of time (Figure 1). At 20 min after the introduction of TMPTMP into a sample of PETA with 34.2 mol % DEA, data for G' have not changed when compared to the same sample without TMPTMP, indicating that at this point a microstructure large enough for detection has not yet formed and the applied stresses within the sample are able to

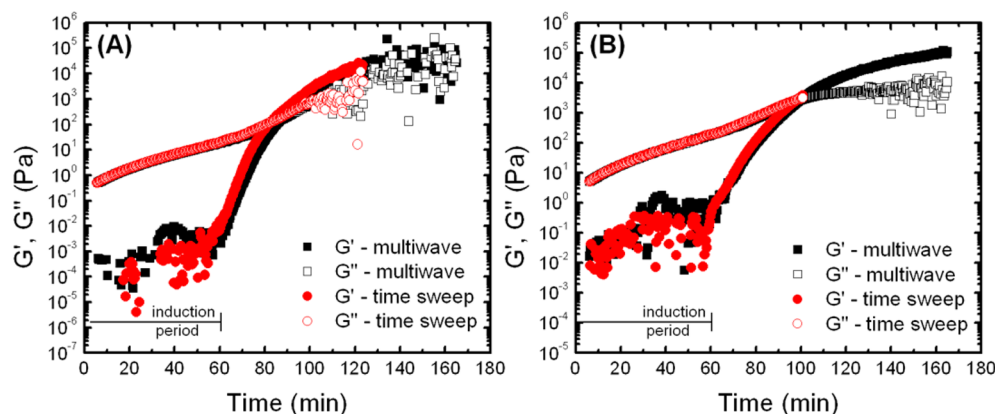


Figure 2. Evolution of the time-dependent elastic (G') and viscous (G'') modulus from a time sweep of PETA with 34.2 mol % DEA, at stress (τ) of 1 Pa and frequency (ω) of (A) 1 rad s^{-1} and (B) 10 rad s^{-1} . Data from FTMS experiments are also shown compared to individual time sweeps performed at the given parameters to demonstrate validity of the FTMS method. The data within the window of interest match very well.

relax to zero. As time progresses, an internal microstructure forms, indicated by the increase in G' , as depicted in Figure 1b. At 72 min after the introduction of TMPTMP, the dynamic moduli have increased by 2 orders of magnitude and are both frequency dependent. The data for G' are less scattered, indicating the presence of a microstructure within the system large enough for detection. At 150 min after adding the trithiol, the magnitude of G' is greater than the magnitude of G'' and independent of frequency, typical of fully cross-linked systems. Throughout the duration of the polymerization, G' has increased almost 7 orders of magnitude, indicative of a highly cross-linked sample.

The previous data offer snapshots of the frequency dependence of the dynamic moduli at three different times without providing detailed information on their evolution. We monitored this sol to gel transition by applying a small stress at constant oscillatory frequency and measuring the change in the dynamic moduli over time. Figure 2 shows the evolution of G' and G'' for a representative sample, PETA with 34.2 mol % DEA, when applying a stress of 1 Pa at frequencies of 1 and 10 rad s^{-1} .

In the early stages of polymerization, G'' is much larger than G' , indicative of a sample in a sol state. At such low viscosities, the elastic character is difficult to detect, indicated by the noisy data for G' . However, around 60 min, G' begins to significantly increase as the polymerized network begins to form. The period of time before the large increase in rate of change of G' is known as the induction period. During this time, although the system is reacting, the small molecules are unable to form a network large enough to respond to the applied stress, as the system is still able to relax within the time of probing. It should be noted during the induction period G' slowly increases, indicating the growth of an elastic network. The length of the induction period was shown to correlate with the composition of DEA, as will be shown in later sections. After the induction period, G' significantly increases as the smaller chains begin to connect and form a microstructural network. Near the point that the dynamic moduli are equal in magnitude, which is also near the gel point, a network of cross-links forms between the top geometry and bottom plate. After this point, G' dominates throughout the duration of the experiment as cross-links continue to form between chains and the solution continues to polymerize. However, the rate of increase for G' slows shortly after the cross over point due to a decrease in the number of

available reactive sites as the reaction nears completion. Over the course of gelation, G' is seen to increase by 7–8 orders of magnitude, revealing the complex nature of this material.

Gel Point Detection. The Winter–Chambon criteria can identify the time required for formation of the critical gel, the system at the gel point. A multiwave approach that generated time sweeps at frequencies of 1, 5, 10, and 20 rad s^{-1} and stress of 1 Pa in a single experiment was used for this purpose. Data within the window of interest from this technique match within 5% with data from individual time sweeps at frequencies of 1 and 10 rad s^{-1} in Figure 2, thereby validating the use of this approach for this system.

Figure 3a shows $\tan \delta$ values for PETA with 34.2 mol % DEA obtained using the multiwave technique, plotted as a function of time for varying frequencies, 1, 5, 10, and 20 rad s^{-1} . In this graph, according to the Winter–Chambon criterion, the point of intersection of $\tan \delta$ represents the moment at which $\tan \delta$ is independent of frequency corresponding to the gel point. For our sample we find the gel time to be approximately 75 min, corresponding to a $\tan \delta$ value of about 20 and a relaxation exponent, n , of 0.97 as calculated using eq 1.

In addition to the convergence of the loss tangent at the gel point, the dynamic moduli also show the same frequency dependence; i.e., both G' and G'' scale as ω^n . This relationship is demonstrated by identical slopes for the moduli in a frequency sweep taken at a time equal to the gel point. As shown in Figure 3b, a frequency sweep at the gel point also shows the slope of the dynamic moduli to be equal to the calculated relaxation exponent. For systems with $n > 0.5$, the gel point has been shown to occur before the $G'-G''$ crossover point in a time sweep, which is seen in this system.

Bonino et al. identified an alternative empirical method to characterize the onset of gelation by monitoring the sample strain during cross-linking for a photo-cross-linkable alginate system.²⁹ When the sample approaches the gel point, the strain rapidly decreases as a result of the increase in modulus. The gel point is then estimated by a minimum in the derivative of log strain with respect to time. By slightly altering the aforementioned method, we are able to identify the gel point of the thiol–acrylate system. Figure 4 shows the change in sample strain over time of PETA with 34.2 mol % DEA for frequencies of 1, 5, 10, and 20 rad s^{-1} . At the onset of gelation as determined by the Winter–Chambon criteria (shown as a vertical line in Figure 4a), the sample strain decreases rapidly.

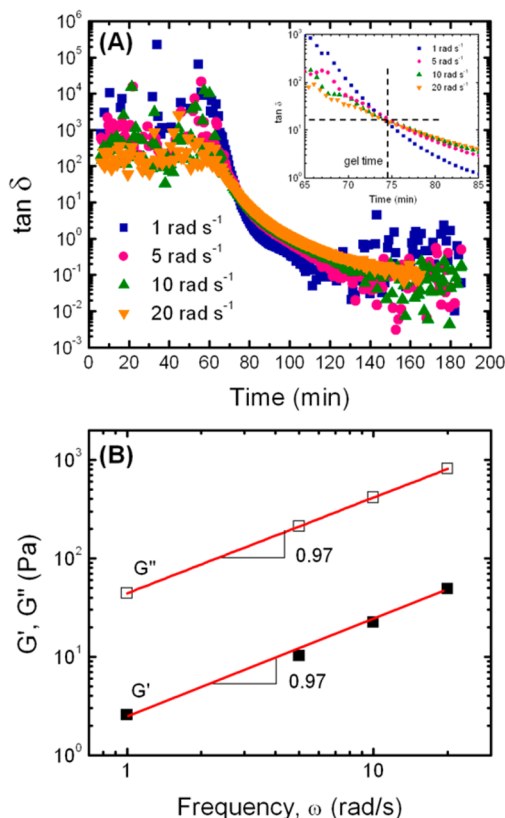


Figure 3. (A) Variation of $\tan \delta$ over time for PETA with 34.2 mol % DEA at frequencies of 1, 5, 10, and 20 rad s^{-1} measured using the multiwave technique. The four curves intersect at the gel point (75 min), indicating that $\tan \delta$ is independent of frequency. Data also correspond to a $\tan \delta$ value of 20. (B) Frequency spectrum at the gel point (75 min) for PETA with 34.2 mol % DEA. The slopes of G' and G'' are parallel, with slopes equal to 0.97. This value represents the relaxation exponent, n , characterizing the frequency-dependent behavior of the dynamic moduli, i.e., $G' \sim G'' \sim \omega^n$.

This region of change provides a window for determining the gel point of the system. Since polymerization begins once the trithiol is introduced, the sample strain decreases over time. However, once the critical gel is formed, the rate of change in the sample strain decreases significantly. By extrapolating lines that follow the change in slope in the data, the gel point may be estimated by the intersection, shown in Figure 4B. Using this technique, we are within 10% of the gel point identified using the Winter–Chambon criteria. Interestingly, Bonino et al. found the empirical approach only worked for low frequencies ($<1 \text{ rad s}^{-1}$);²⁹ however, this altered approach is shown to properly identify the gel point of this system for frequencies up to 20 rad s^{-1} . We find this technique provides a quick means of identifying a gelation window, while complementing the aforementioned $\tan \delta$ method. This approach may thus be of further interest as we show it extends beyond photo-cross-linkable systems.

Effect of *In Situ* Catalyst Concentration. Dynamic oscillatory rheology experiments and the Winter–Chambon method were employed on samples with varying amine concentrations in order to investigate the effects of the *in situ* catalyst concentration on the gel time and gel properties. Modulating the amount of DEA added into the system provides control over the concentration of *in situ* catalyst/comonomer formed by the reaction between DEA and PETA, which

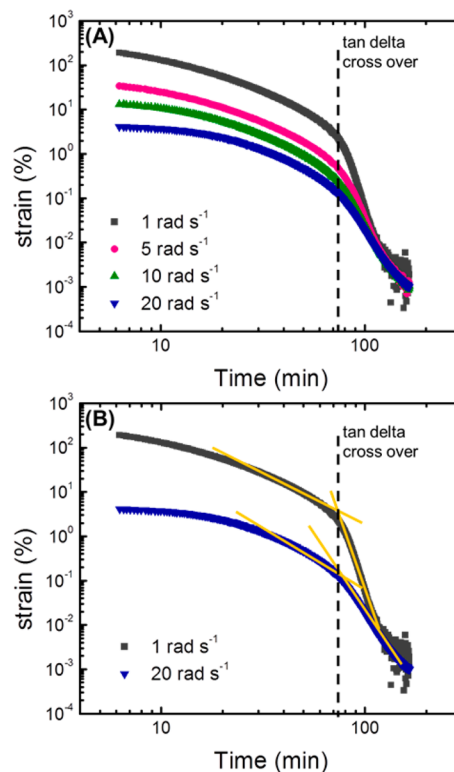


Figure 4. (A) Strain on PETA with 34.2 mol % DEA over time throughout the polymerization reaction at 1, 5, 10, and 20 rad s^{-1} and a constant stress (τ) of 1 Pa. At the onset of gelation (75 min) as determined by Winter–Chambon criteria, the relationship between strain and time changes dramatically, indicated by significant changes in slope. (B) An empirical approach can be used to estimate the gel point by extrapolating lines following the slope of the change in percent strain of the sample over time. The gel point can be estimated by the intersection of the lines. This empirical approach applies to frequencies as great as 20 rad s^{-1} .

converts trifunctional acrylates into difunctional acrylates. The gel points as a function of DEA concentration identified by the Winter–Chambon method are shown in Figure 5.

A minimum in gel time is seen as a function of amine concentration consistent with the observation of Bounds et al.¹⁸ obtained using a crude bubble entrapment method for

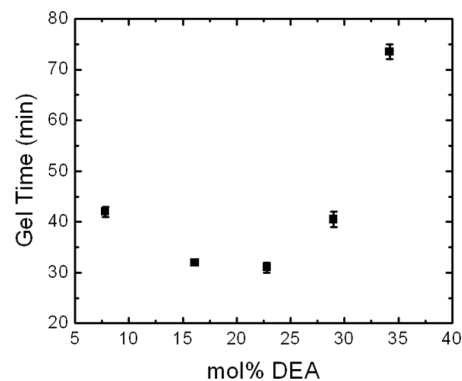


Figure 5. Calculated gel points, from the Winter–Chambon method, as a function of mol % DEA, where mol % DEA is calculated as the ratio of moles of amine groups to moles of acrylate groups. A minimum in gel time is seen due to the number of available reaction sites.

determining gel point. The time required for gelation decreases as the concentration of catalyst increases, up to 22.8 mol % DEA, which is expected. However, as the DEA concentration continues to increase, the time required for gelation increases as well. Bounds et al. attribute this change to a higher critical extent of conversion,¹⁸ which is the conversion required before a gel microstructure can form. The extent of reaction at the gel point (p_c) can be calculated using the statistical approach developed by Flory and Stockmayer.³⁰ Since this system is comprised of a trifunctional acrylate, difunctional acrylate catalyst/comonomer, and trifunctional thiol, we use the following equation for a system with two functional groups that serve as branching units:

$$p_c = \frac{1}{[r(f_{w,\text{acrylate}} - 1)(f_{w,\text{thiol}} - 1)]^{1/2}}$$

where r is the stoichiometric ratio of the thiol to acrylate functional groups, which is equal to one for this system as an acrylate functional group reacts directly with a thiol functional group. Additionally, $f_{w,\text{acrylate}}$ represents the weight-average functionality of the monomers containing acrylate functional groups, and $f_{w,\text{thiol}}$ represents the weight-average functionality of the thiol monomer. In agreement with previous reports,¹⁸ we find that the concentration of DEA and the critical extent of reaction are directly proportional (Figure 6).

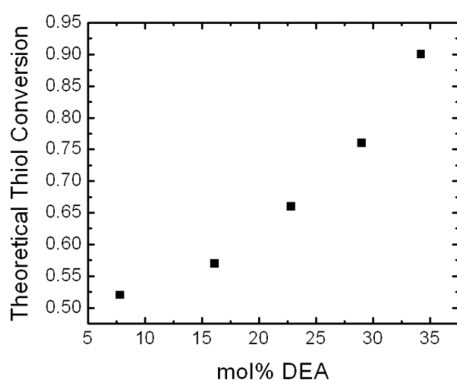


Figure 6. Theoretical thiol conversion at the gel point calculated using the Flory–Stockmayer statistical approach as a function of mol % DEA. As the amine concentration increases, a higher conversion is required for the system to gel.

This relationship is due to a decrease in acrylate functionality caused by the increase in DEA concentration and can be used to explain the minimum observed in gel time (Figure 5). As the amine concentration increases, a higher percentage of PETA molecules react to form difunctional acrylates, decreasing the overall acrylate functionality of the system. Thus, a higher percent conversion is required before a significant gelled network can form. The decrease in overall acrylate functionality and increase in the percent conversion required for gelation is directly reflected in the time required for gelation. For samples containing catalyst concentration less than 22.8 mol %, the gel point decreases due to an increase in catalyst concentration. However, at catalyst concentrations greater than 22.8 mol %, the benefit gained from an increase in catalyst concentration is negated by the decrease in acrylate functionality. For these samples, greater than 75% of the thiol functional groups in the system must react before a gelled microstructure can form. Thus, the time required for gelation increases.

We are able to verify the theoretical critical conversion predicted by Flory and Stockmayer using rheological techniques to identify the gel point and Fourier transform infrared spectroscopy (FTIR) to monitor the thiol conversion. FTIR data show propagation of the thiol–acrylate reaction over time (Figure 7). The conversion at the gel point for PETA with 16.1 mol % DEA and 29 mol % DEA is 0.55 and 0.71, respectively. Both values match well with the theoretical critical conversion at the gel point, predicted as 0.57 and 0.76 for PETA with 16.1 mol % DEA and 29 mol % DEA, respectively. Slight discrepancies in the theoretical and experimental values may be attributed to the assumption that all functional groups of the same type are equal in reactivity and error in the FTIR conversion calculations as the reaction may propagate during initial measurements. This agreement further validates the accuracy of the Winter–Chambon criteria for gel point detection in a polymerizing system with an *in situ* catalyst species.

Using rheological techniques and FTIR, we are able to correlate the thiol conversion with the elastic modulus of the system, providing a means to analyze the growth of the microstructure not only in terms of time but also in terms of degree of conversion. Figure 7a shows the thiol conversion, adapted with permission from Bounds et al.,¹⁸ and G' as a function of time for PETA with 16.1 mol % DEA. In the initial stages of the reaction, the percent conversion of thiol increases rapidly, reaching a conversion of roughly 0.55 within 30 min after the addition of TMPTMP. However, during this period of time, the elastic modulus has no appreciable value. Shortly after the gel point, the magnitude of G' increases rapidly. This delay in growth of G' can be explained by recalling the theoretical value of $p_c = 0.57$. This value indicates that the reaction must proceed to a critical conversion before G' is detectable, as seen in Figure 7c. G' is negligible at conversions less than p_c . However, after this point, G' increases roughly 2.5 orders of magnitude as the thiol conversion shows only a 10% increase. The same trend is shown for PETA with 29 mol % DEA in Figures 7b and 7d. Until the critical conversion of 0.71 is reached, which matches well with the theoretical value of $p_c = 0.76$, G' has no appreciable value but grows very rapidly after the critical conversion. These data verify our previous hypothesis that the minimum in gel point is related to an increase in percent conversion required for gelation. Relating the magnitude in G' and percent conversion has also been shown for a PDMS system³¹ and a thiol–allyl system.³² Additionally, these features are indicative of the suggested step-growth mechanism, where high conversion is required before a highly cross-linked network is formed. At lower conversions, shorter oligomers are able to relax within the time scale of the experiment. At the critical conversion, p_c , the larger microstructure is unable to relax fully during the time scale of the experiment and G' can be detected. G' will then continue to grow rapidly as the reaction proceeds to completion.

We have demonstrated that modulating the amine concentration can affect the time required for gelation, but it is also important to analyze the state of the cross-linking system at the gel point. Winter and Chambon have shown that rheological data, particularly the relaxation exponent, n , can be used to investigate the microstructure of the critical gel.²⁴ The relaxation exponent for systems of varying amine concentration can be calculated using eq 1. Previous literature calculated relaxation exponents of 0.8 and 0.81–0.82 for trifunctional and tetrafunctional thiols, respectively, in a photoinitiated thiol–

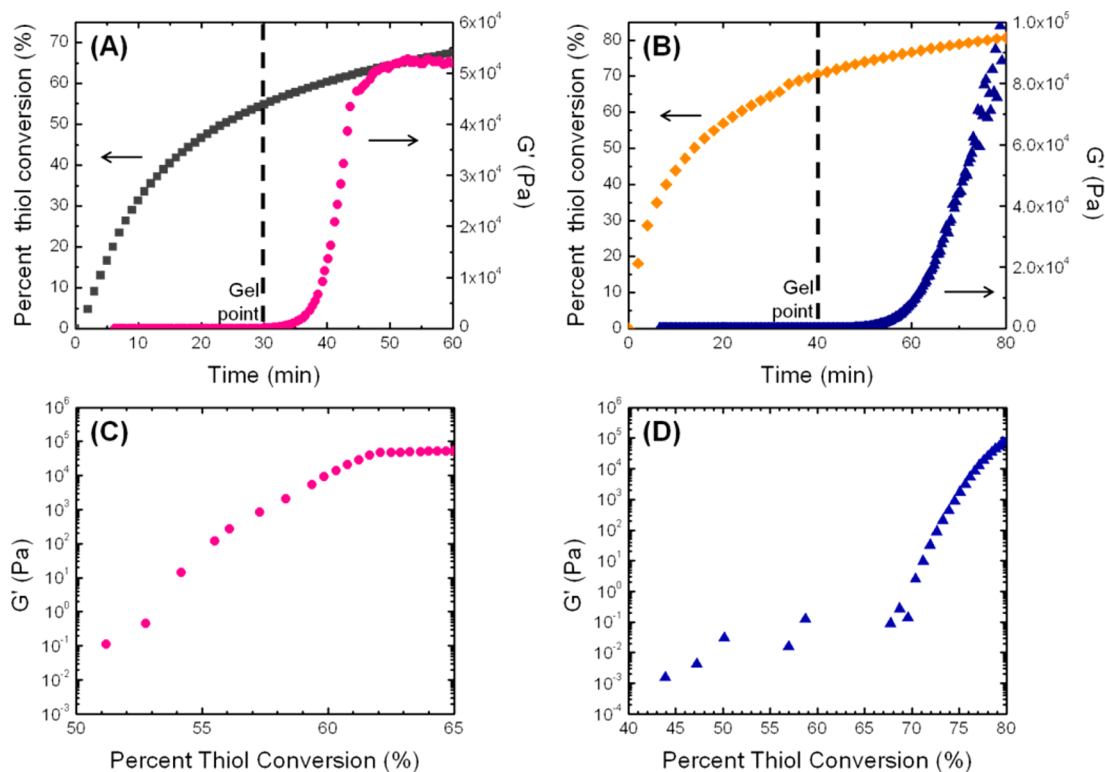


Figure 7. Percent thiol conversion and evolution of elastic modulus (G') shown over time for PETA with (A) 16.1 mol % DEA (■, ●) and (B) 29 mol % DEA (◆, ▲). G' plotted against percent thiol conversion for PETA with (C) 16.1 mol % DEA and (D) 29 mol % DEA. Percent conversions of 55% and 71%, respectively, are required before the elastic moduli have any appreciable value.

allyl reaction.²⁷ However, no in-depth rheological gelation studies have been performed for thiol–acrylate systems, specifically systems incorporating an *in situ* catalyst/comonomer. The exponent values observed for this system are very high, ranging between 0.97 and 0.98 for all samples. It is typical to find values of $n > 0.5$ for cross-linked systems with $n = 0.5$ found only for systems in specific stoichiometric conditions, corresponding to a gel time occurring at the time of the G' and G'' crossover.^{25,33} Winter has shown for systems where $n > 0.5$ such as ours the gel point occurs before the G' , G'' crossover point,²³ indicating a critical gel with a greater viscous modulus than elastic modulus. Results for our system are consistent and expected due to the lack of elastic character in the pregel state. Some researchers have attempted to establish a definitive relationship between the relaxation exponent and molecular weight of the prepolymer. Izuka et al. showed that the relaxation exponent increased as the prepolymer molecular weight decreased for end-linking polycaprolactone (PCL). A relaxation exponent value as high as 0.91 was calculated for PCL of number-average molecular weight equal to 2000.³⁴ Additionally, Scanlan et al. calculated a relaxation exponent of 0.92 for a system of end-linking medium chained PDMS with excess diluents.³⁵ We believe the high value of n may be due to low molecular weight prepolymer. Since the molecular weight of monomers in our system is extremely low, approximately 300–400 g/mol, resulting in a pregel with negligible elastic character, the high relaxation exponent is not unexpected.

Another parameter used to analyze the microstructure of the critical gel is the fractal dimension, d_f . It has been shown that the power law relationship demonstrated between G' , G'' and frequency at the gel point is due to the self-similar nature of the critical gel.³⁶ The self-similar nature refers to the fact that if a

portion of the critical gel were magnified, the overall structure would resemble the original piece, no matter the magnification or size of the original portion. This self-similarity is quantified using the fractal dimension which has been shown to relate the radius of gyration (spatial size, R), and molecular weight of the polymer as follows:³⁷

$$R^{d_f} \sim MW$$

Assuming excluded-volume effects are screened, the fractal dimension can be calculated using the equation

$$n = \frac{d(d + 2 - 2d_f)}{2(d + 2 - d_f)}$$

where n is the relaxation exponent at the gel point and d the space dimension 3.^{25,37} The same fractal dimension of 1.3 was calculated for all systems investigated. Although such low fractal dimensions have not been reported for polymeric systems, a fractal dimension of 1.3 has been observed in nature to represent tree branches, root systems, and clouds.³⁶ Low fractal dimensions, yet values higher than our system, have been associated with open structures,³⁵ the polymerization of small molecules, and systems with many cross-linking defects.^{22,37,38} All reactants in the system are small molecules, and the *in situ* catalyst comonomer contains an amine functional group which truncates chain growth in that direction, as the polymerization proceeds between the acrylate and thiol groups. These factors may promote defects in the cross-linked network. Considering these attributes, a low fractal dimension should not be unexpected.

Utilizing the Boltzmann inversion³⁹ coarse-graining method along with DMD⁴⁰ simulations in the EMBLEM package developed by Curtis and Hall,⁴¹ we are able to qualitatively

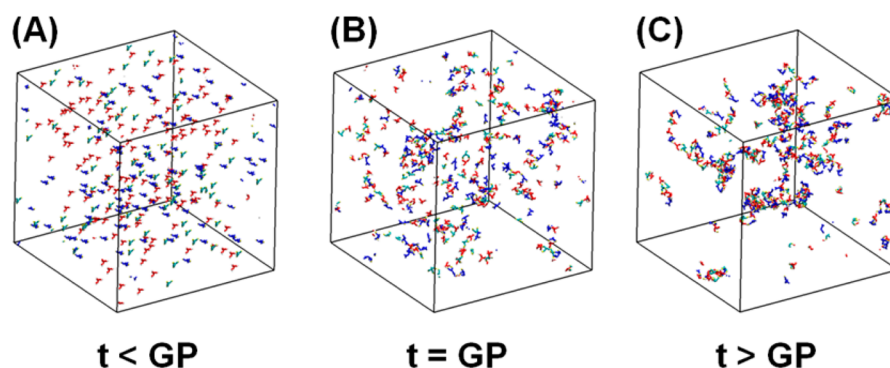


Figure 8. Simulation snapshots of PETA with 16.1 mol % DEA at (A) 0%, (B) 57%, and (C) 95% thiol conversion. The catalyst is pictured in blue, PETA is pictured in cyan, and TMPTMP is pictured in red with all thiol groups in white and all acrylate groups in yellow. As the reaction continues, the prepolymer monomers can be seen reacting together, forming a cross-linked network.

verify the state of the critical gel of PETA containing 16.1 mol % DEA and, further, quantitatively verify the fractal dimension and theoretical critical extent of reaction (p_c). The model uses the Boltzmann inversion coarse-graining method to obtain realistic geometry configurations and interactions between coarse-grained functional groups. To mimic the step growth polymerization of PETA, thiol functional groups were labeled as reactive if they had an excluded-volume reaction with the nitrogen from the amine group on the *in situ* catalyst, thereby mimicking the deprotonation of the thiol group by the catalyst. If a specific thiol and acrylate group had an excluded-volume interaction and had been previously designated as reactive, a permanent bond was formed between the two sites. At low conversions, the simulation shows the formation of small clusters, agreeing well with previously discussed rheological data, shown in Figure 8a. As the reaction approached the theoretical critical extent of reaction, calculated as 0.57 using Flory–Stockmayer’s statistical approach, larger chains began to form. The extent of reaction was calculated as the ratio of thiolene bonds in the simulation to the theoretical maximum amount of thiolene bonds. In order to characterize the system at the gel point, further thiolene bonding past an extent of reaction of 0.57 was prevented. In Figure 8b, the polymer chains have begun to span into a three-dimensional area, characteristic of the critical gel. However, it should be noted that the simulation box contains a small piece of what is typically examined in a rheological sample. Therefore, at the calculated gel point the largest polymer chain does not span the entire length of the simulation box. When the reaction nears completion, the system contains primarily cross-linked polymer chains (Figure 8c).

Using the relationship between the radial distribution function and fractal dimension established by Kieffer and Angell,⁴² we are able to calculate the fractal dimension of the simulated system at the gel point as 1.34, which is in agreement with the experimental values. The computer simulations allow for the capturing of a transient state, such as the gel point and critical gel, allowing for the validation of experimental characteristics. Interestingly, the relaxation exponent and the fractal dimension remain unaffected by changes in the amine concentration.

Figure 9 contains rheological time sweeps for all systems investigated. As can be seen, the elastic modulus plateaus at approximately the same value despite changes in amine concentration. The only change observed is the length of the induction period, which relates back to the previous discussion

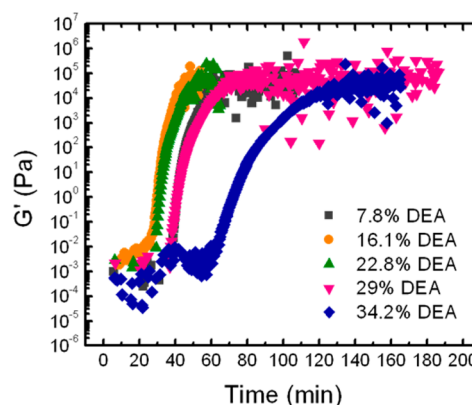


Figure 9. Evolution of the elastic (G') and viscous (G'') moduli over time at frequency (ω) of 1 rad s^{-1} and stress (τ) of 1 Pa of samples with 7.8, 16.1, 22.8, 29, and 34.2 mol % DEA.

regarding the trade-off between an improvement in reaction speed due to increased catalyst concentration and higher critical conversions required for gelation. Since the relaxation exponent is also independent of the amine concentration, we conclude that the cross-linking mechanism remains unaffected by changes in the concentration of *in situ* catalyst.⁴³ This provides the ability to tune the gel time of the system by modulating the amine concentration without affecting the formation mechanism or spatial size of the critical gel.

SUMMARY

We have demonstrated the applicability of dynamic rheology together with a multiwave technique and the Winter–Chambon criteria for examining the gelation of a novel thiol–acrylate system where an *in situ* catalyst is incorporated into the cross-linked network. Using this approach, we were able to probe the evolving rheological properties and relate the macroscopic properties to the gel time and characteristics of the critical gel, such as the fractal dimension. We also investigated the effect of amine concentration from 7.8 mol % DEA to 34.2 mol % DEA on the gelation mechanism, properties of the critical gel, and gel times.

The gel times for all systems investigated ranged from as short as 30 min for 16.1 mol % DEA to as long as 75 min for 34.2 mol % DEA. Initially, the time required for gelation decreased as the amine concentration increased up to 22 mol % DEA. At concentrations greater than 22 mol % DEA, the time required for gelation increased. We attribute this trend to a

decrease in the overall acrylate functionality, requiring a higher thiol conversion for gelation to occur. Rheological techniques in combination with FTIR were used to calculate the conversion at the gel point for PETA with 16.1 mol % DEA and 29 mol % DEA. The experimental thiol conversion of 0.55 and 0.71 at the gel point matched well with the theoretical conversions calculated using the statistical approach developed by Flory and Stockmayer.

The value of the relaxation exponent, n , for all systems investigated was approximately 0.97, yielding a fractal dimension of 1.3. The high value of n can be attributed to the low molecular weight of the prepolymer materials, resulting in a lack of any significant elastic character in the pregel state. As such, the gel time occurring before the G' , G'' crossover point was not unexpected. Such low fractal dimensions have not been reported for polymeric systems but have been observed in nature. Interestingly, we found the final elastic modulus to be equal for all systems investigated as well. Since the relaxation exponent was independent of changes in the amine concentration, we conclude that the reaction mechanism remained the same for all systems. Changes in the amine concentration, and thus the *in situ* catalyst concentration, seem to only affect the rate of reaction and time required for gelation. Altering the amine concentration changes the time required for gelation without affecting the cross-linking mechanism or development of the critical gel. This provides facile control over the gelation time without sacrificing the integrity of the critical gel, which would be imperative for applications such as *in situ* gelation in the biomedical field.

AUTHOR INFORMATION

Corresponding Author

*E-mail: khan@ncsu.edu (S.A.K.).

Notes

The authors declare no competing financial interest.

ACKNOWLEDGMENTS

The authors acknowledge Dr. Christopher Bounds for his help with FTIR analysis and assistance in development of the thiol-acrylate system.

REFERENCES

- (1) Hoyle, C. E.; Bowman, C. N. *Angew. Chem., Int. Ed.* **2010**, *9*, 1540–1573.
- (2) Cramer, N.; Reddy, S.; Cole, M.; Hoyle, C.; Bowman, C. *J. Polym. Sci., Polym. Chem.* **2004**, *22*, 5817–5826.
- (3) Cramer, N.; Bowman, C. *J. Polym. Sci., Polym. Chem.* **2001**, *19*, 3311–3319.
- (4) van Berkel, K. Y.; Hawker, C. J. *J. Polym. Sci., Polym. Chem.* **2010**, *7*, 1594–1606.
- (5) Lee, T. Y.; Bowman, C. N. *Polymer* **2006**, *17*, 6057–6065.
- (6) Bounds, C. O.; Goetter, R.; Pojman, J. A.; Vandersall, M. *J. Polym. Sci., Polym. Chem.* **2012**, *3*, 409–422.
- (7) Hu, G.; Bounds, C.; Pojman, J. A.; Taylor, A. F. *J. Polym. Sci., Polym. Chem.* **2010**, *13*, 2955–2959.
- (8) Khire, V. S.; Kloxin, A. M.; Couch, C. L.; Anseth, K. S.; Bowman, C. N. *J. Polym. Sci., Part A: Polym. Chem.* **2008**, *20*, 6896–6906.
- (9) Besson, E.; Gue, A.; Sudor, J.; Korri-Youssoufi, H.; Jaffrezic, N.; Tardy, J. *Langmuir* **2006**, *20*, 8346–8352.
- (10) van der Ende, A.; Croce, T.; Hamilton, S.; Sathiyakumar, V.; Harth, E. *Soft Matter* **2009**, *7*, 1417–1425.
- (11) Binici, B.; Fortenberry, D.; Leard, K.; Molden, M.; Olten, N.; Popwell, S.; Pojman, J. *J. Polym. Sci., Part A: Polym. Chem.* **2006**, *4*, 1387–1395.
- (12) Pojman, J.; Varisli, B.; Perryman, A.; Edwards, C.; Hoyle, C. *Macromolecules* **2004**, *3*, 691–693.
- (13) Rydholm, A.; Bowman, C.; Anseth, K. *Biomaterials* **2005**, *22*, 4495–4506.
- (14) Rydholm, A. E.; Held, N. L.; Bowman, C. N.; Anseth, K. S. *Macromolecules* **2006**, *23*, 7882–7888.
- (15) Rydholm, A. E.; Held, N. L.; Benoit, D. S. W.; Bowman, C. N.; Anseth, K. S. *J. Biomed. Mater. Res., Part A* **2008**, *1*, 23–30.
- (16) Chan, J. W.; Wei, H.; Zhou, H.; Hoyle, C. E. *Eur. Polym. J.* **2009**, *9*, 2717–2725.
- (17) Chan, J. W.; Hoyle, C. E.; Lowe, A. B.; Bowman, M. *Macromolecules* **2010**, *15*, 6381–6388.
- (18) Bounds, C. O.; Upadhyay, J.; Totaro, N.; Thakuri, S.; Garber, L.; Vincent, M.; Huang, Z.; Hupert, M.; Pojman, J. A. *ACS Appl. Mater. Interfaces* **2013**, *5*, 1643–1655.
- (19) Prasath, R. A.; Gokmen, M. T.; Espeel, P.; Du Prez, F. E. *Polym. Chem.* **2010**, *5*, 685–692.
- (20) Garber, L.; Chen, C.; Kilchrist, K. V.; Bounds, C.; Pojman, J. A.; Hayes, D. *J. Biomed. Mater. Res., Part A* **2013**, n/a–n/a.
- (21) Salinas, C. N.; Anseth, K. S. *Macromolecules* **2008**, *16*, 6019–6026.
- (22) Winter, H. H. Physical and Chemical Gelation. In *Encyclopedia of Materials: Science and Technology*; Buschow, K. H. J., Cahn, R. W., Flemings, M. W., Ilshner, B., Kramer, E. J., Mahajan, S., Eds.; Elsevier: New York, 2001; pp 6991–6999.
- (23) Winter, H. H. *Polym. Eng. Sci.* **1987**, *22*, 1698.
- (24) Chambon, F.; Winter, H. H. *J. Rheol.* **1987**, *8*, 683–697.
- (25) Winter, H. H.; Chambon, F. *J. Rheol.* **1986**, *2*, 367–382.
- (26) Raghavan, S.; Chen, L.; McDowell, C.; Khan, S.; Hwang, R.; White, S. *Polymer* **1996**, *26*, 5869–5875.
- (27) Chiou, B.; English, R.; Khan, S. *Macromolecules* **1996**, *16*, 5368–5374.
- (28) Walls, H.; Caines, S.; Sanchez, A.; Khan, S. *J. Rheol.* **2003**, *4*, 847–868.
- (29) Bonino, C. A.; Samorezov, J. E.; Jeon, O.; Alsberg, E.; Khan, S. A. *Soft Matter* **2011**, *24*, 11510–11517.
- (30) Odian, G. Crosslinking. In *Principles of Polymerization*; John Wiley & Sons: New York, 1991; pp 103–104–112.
- (31) Venkataraman, S. K.; Coyne, L.; Chambon, F.; Gottlieb, M.; Winter, H. H. *Polymer* **1989**, *12*, 2222–2226.
- (32) Chiou, B.; Khan, S. *Macromolecules* **1997**, *23*, 7322–7328.
- (33) Elbrahmi, K.; Francois, J.; Dupuis, D. *Rheol. Acta* **1995**, *1*, 86–96.
- (34) Izuka, A.; Winter, H. H.; Hashimoto, T. *Macromolecules* **1992**, *9*, 2422–2428.
- (35) Scanlan, J. C.; Winter, H. H. *Macromolecules* **1991**, *1*, 47–54.
- (36) Feder, J. *Fractals*; Plenum Press: New York, 1988.
- (37) Muthukumar, M. *Macromolecules* **1989**, *12*, 4656–4658.
- (38) Ponton, A.; Barboux-Doeuff, S.; Sanchez, C. *Colloids Surf., A* **2000**, *1–3*, 177–192.
- (39) Reith, D.; Putz, M.; Muller-Plathe, F. *J. Comput. Chem.* **2003**, *13*, 1624–1636.
- (40) Alder, B. J.; Wainwright, T. E. *J. Chem. Phys.* **1959**, *2*, 459–466.
- (41) Curtis, E. M.; Hall, C. K. *J. Phys. Chem. B* **2013**, *117*, 5019–5030.
- (42) Kieffer, J.; Angell, C. A. *J. Non-Cryst. Solids* **1988**, *1–3*, 336–342.
- (43) Izuka, A.; Winter, H. H.; Hashimoto, T. *Macromolecules* **1994**, *23*, 6883–6888.